Egyptian Informatics Journal 24 (2023) 100407

Contents lists available at ScienceDirect

Egyptian Informatics Journal

journal homepage: www.sciencedirect.com

Reverse polarity optical Orthogonal frequency Division Multiplexing for High-Speed visible light communications system

Ghaida Muttashar Abdulsahib [a], Dhana Sekaran Selvaraj [b], A. Manikandan [c], SatheeshKumar Palanisamy [d,*], Mueen Uddin [e], Osamah Ibrahim Khalaf [f], Maha Abdelhaq [g], Raed Alsaqour [h]

[a] Department of Computer Engineering, University of Technology, Baghdad, Iraq
[b] Department of ECE, Sri Eshwar College of Engineering, Coimbatore, Tamil Nadu 641202, India
[c] Dept. of ECE, College of Engineering and Technology, SRM Institute of Science and Technology, Kattankulathur, Chennai, 603203
[d] Department of ECE, Coimbatore Institute of Technology, Coimbatore, Tamil Nadu 641014, India
[e] College of Computing and IT, University of Doha for Science and Technology, 24449 Doha, Qatar
[f] Al-Nahrain University, Al-Nahrain Renewable Energy Research Center, Baghdad, Iraq
[g] Department of Information Technology, College of Computer and Information Sciences, Princess Nourah bint Abdulrahman University, P.O. Box 84428, Riyadh 11671, Saudi Arabia
[h] Department of Information Technology, College of Computing and Informatics, Saudi Electronic University, Riyadh 93499, Saudi Arabia

ARTICLE INFO

Keywords:
Visible Light Communication (VLC)
Reverse Polarity OFDM
Berlekamp–Massey algorithm (BMA)
signal to noise ratio (SNR)
bit error rate (BER)

ABSTRACT

The radio frequency spectrum, which has been steadily getting smaller, is under pressure from growing cellular data traffic. A more dependable communication channel is required. To setup the communication medium, VLC uses LED illumination. In order to increase network throughput, the goal of this study is to analyze and model signal conditioning techniques in the visible spectrum. VLC technology offers synchronized illumination of LED lamps as well as wireless broadband connectivity. Using the real-valued O-OFDM baseband signal, optical orthogonal frequency division multiplexing (O-OFDM) offers a viable modulation option for very-low-bit-rate (VLC) systems to modulate the optical carrier's instantaneous power to attain gigabit data rates. However, one important design difficulty preventing VLC from being commercialized is how to combine industry-favored pulse width modulation (PWM) dimming technology while retaining a dependable, broadband connection. In this paper, Reverse Polarity optical orthogonal frequency division multiplexing (RPO-OFDM) is proposed as a new signal format for combining the fast O-OFDM contact signal with the comparatively slow PWM dimming signal, as both signals contribute to the illuminative brightness of the LED. The average SNR, additional testing demonstrates that the suggested method outperforms the Asymmetrically clipped optical OFDM (ACO), Optimized Flipped Optical (OFO) and DC biased optical OFDM (DCO), and algorithms in similar operating conditions.

1. Introduction

Indicators of various technological, economic, governmental, and institutional aspects of global integration, are all influenced by wireless communications. In order to provide seamless wireless coverage and capacity, alternative spectrum integration is necessary because to the abuse and congestion of the existing radio spectrum caused by the technological revolution and the increase in global population density. Infrastructure for high-speed wireless communication must be built as demand for wireless communication services grows. In comparison to fourth-generation technologies, which have a data transfer rate of 30Mbps [2], first-generation technologies have a data transfer rate of only 2.4kbps [1]. The fifth generation of technology is being intended to achieve a minimum of 1 Gbps [3] in light of the escalating demands of a data-scarce society. This electromagnetic spectrum has the potential for high-throughput communication and has a frequency bandwidth that ranges from 430 THz to 790 THz [4]. Despite these benefits, the nature of frequency bands precludes the direct application of methodologies for RF design and necessitates some creative thinking in signal processing. This is due to the limited signal processing that is required for the

* Corresponding author.
E-mail address: satheeshkumar.p@cit.edu.in (S. Palanisamy).

https://doi.org/10.1016/j.eij.2023.100407
Received 7 January 2023; Received in revised form 15 July 2023; Accepted 26 September 2023
Available online 10 October 2023

transmission and reception of visible light signals, which must be intensity-modulated during transmission. This restriction can be somewhat avoided by using non-negative real-valued unipolar signals rather than complex-valued bipolar signals that have been processed for RF spectrum applications [5].Fig. 1..

Even at low brightness levels, optical data transmission must be reliable. One of the key components of a VLC system is its lighting quality power and consumption. The development of a reliable and effective darkening control mechanism is required to adjust the brightness without interfering with the communication medium. Dimming control was added to VLC primarily to reduce the amount of energy used by the LEDs and to enhance user ease. In wireless communication, LEDs serve as both a light source and a medium. Light levels between 200 and 1000 lx [6] are needed for a typical office setting. So, it's best to keep the lights in this range. The VLC system suffers from dimming control. The average signal strength will be lessened when the communication medium is set up after the LED lights had been dimmed. Additionally, it is feasible to decrease the data rate while simultaneously increasing BER and SNR. Therefore, offering and creating an appropriate solution for VLC darkening control is a challenge and a current research area.

Previous single-carrier modulation techniques have been successful in reducing the issues with frequency selection of the transmission process [7] that arise in widely dispersed and multipath-driven radio channels, allowing for high throughput/data rates. Singular carrier with frequency-domain power ratio has recently been developed [8]. Despite the fact that these modulation techniques are well suited for RF applications, the RF spectrum's constrained bandwidth restricts the potential data speeds in this area, necessitating the usage of alternate frequencies like visible light spectrum bands at the moment. Maturity in radio frequency technologies allows for the usage of visible light communication (VLC) deployments to provide faster data speeds due to the visible spectrum's inherent larger bandwidth features [9]. Being forced to deal with unipolar signals, as opposed to complex, bipolar RF signals, is a key issue when dealing with signals in the visible range. Due to the fact that pre-existing concepts are not directly relevant, this aspect of the signal necessitates a certain amount of inventiveness in processing and channel estimate. Consider signal transmission in the visible spectrum, a crucial component in OFDM applications, fusing the potential of developed/crowded radio bands with alternative bands like the visible spectrum to boost data speeds. The development of a high throughput high-performance channel model is ongoing [10].

The driving signal for the LEDs must be a real positive signal [11,12]. Since O-OFDM is used for VLC optical communication using real and positive signals, the suggested digital PWM darkening control method employs this technique. To produce true and positive signals, restrict to Hermitian symmetry from the input of the OFDM Inverse Fast Fourier Transform (IFFT). To modulate the data into light intensity, the study used a kind of O-OFDM called RPO-OFDM. A somewhat slow PWM dimming signal that uses RPO-OFDM as a carrier is used. In order to use the complete PWM pulse in the off state, RPO-OFDM inverts the polarity. This guarantees continuous data transmission. The desired dimming ratio is used to determine the PWM duty cycle. For carrier and dimming signals, PWM pulses are appropriate. Improved outcomes on the BER side are obtained by concatenating FEC codes, such as Reed Solomon convolutional coding (RS-CC). To identify the minimal light intensity necessary for effective communication utilizing VLC technology, a number of tests and comparisons were made in terms of BER (relative to SNR side).

2. Contribution

To obtain Hermitian symmetry, the genuine and real positive signal is obtained by limiting the input to IFFT of OFDM multiplex. Reversal of Optical Polarity This study uses OFDM (RPO-OFDM), a kind of O-OFDM, to modulate light intensity data.

In this paper, Reverse Polarity O-OFDM (RPO-OFDM) is proposed as a new signal format for combining the fast O-OFDM contact signal with the comparatively slow PWM dimming signal, as both signals contribute to the effective brightness of the LED.

The PWM pulse serves as both a fader and a bus signal. Reed Solomon-Convolutional Coding series have produced better BER (signal-to-noise ratio) outcomes. Several studies and comparisons in terms of BER (relative SNR) have been conducted to identify the minimum light intensity required for successful communication with VLC technology.

When the signal clipping is not prominent, the employment of carrier BCS offers a very data stream on the BER of the ACO-OFDM signal, according to the simulated BER.

Literature Survey.

By eliminating inter-symbol interference (ISI) and ICI, OFDM is able to achieve the guard time between adjacent symbols, ensure the orthogonality of sub-carriers, and replace single carrier [11]. With single-carrier technology, channel impairments and spectrum waste due to dispersion effects in the communication line are a significant issue. OFDM systems are notoriously challenging to implement the increase in SNR [12] is bottlenecked at high PAPR, making the transmitter front-end extremely complex, even though the performance is comparable under conditions of channel loading and larger data rates are attainable. High bit error rates and subpar RF application performance are caused by these obstacles [13]. The implementation of multicarrier techniques with OFDM in VLC directly addresses these concerns, even though this presumption has long been a subject of academic and industrial research. Due to the unique characteristics of the signal being processed, using multi-carrier schemes in VLC is a crucial consideration in order to achieve high throughput at enhanced SNR and low bit error rate (i.e. requiring direct detection and intensity modulation. It directly results in the adaptation-related steps that are required [14].

Using the visible spectrum as a wireless communication medium is known as visible light communication. Even in dim light, a reliable communication link must be able to be established. The history of dimming control technology is covered in this part to help with the assurance of clear communication in dimly lit areas [15]. For the purpose of controlling LED lighting, analogue dimming employs Continuous Current Reduction (CCR) technology. Dimming is accomplished in a CCR by decreasing the LED voltage, which immediately lowers the current flowing through the LED [16]. As a result, the LED is underdriven, which alters the chromaticity [17]. An objective standard, independent of brightness, known as chromaticity, can be used to determine an LED's colour quality. Because of this, digital PWM dimming eventually took the place of analogue dimming, and LED dimming is accomplished by adjusting the duty cycle.

Recent research efforts are underway to develop editing solutions that handle the integration difficulty with wideband VLC, high-quality lighting, and lighting state management. Only in the "on" state are O-OFDM symbols transferred to the PWM signal in the time domain [18]. The comparatively slow PWM line speed limits the data output in this case. The LED driver current is calculated by multiplying the time domain Optical-Orthogonal Frequency Division Multiplexing signal by the PWM periodic pulse train [19]. Only the "on" state of the PWM

Fig. 1. O-OFDM Transmitter Block Diagram.

Table 1
Summary of the Literature Survey.

Types of OFDM	Method	Limitation
Asymmetrically clipped optical Orthogonal Frequency Division Multiplexing (ACO-OFDM)	To generate genuine non-negative signals for use in IM/DD systems.	If the compatibility to dimming control is to be achieved.
DC-biased optical Orthogonal Frequency Division Multiplexing (DCO-OFDM)	By directly altering the biasing and scaling of the optical OFDM signals,	The implementation of signal shaping is difficult due to the lack of an efficient analytical approach for measuring the bias and scaling coefficient.
Asymmetrically clipped DC biased optical Orthogonal Frequency Division Multiplexing (ADO-OFDM)	The brightness is controlled using a periodic binary brightness control sequence (BCS) with a duty cycle.	The sequence of OFDM signal is high frequency, which is not achievable with standard LED drivers.
Unipolar OFDM (U-OFDM)	A wide darkening range was claimed, but at the expense of significant implementation	Depending on the desired brightness, the durations of the off and on states are configured

signal[20] receives O-OFDM symbols in the time domain [21]. The comparatively slow PWM line speed limits the data output here. Because the PWM frequency of off-the-shelf LED drivers is in kHz, this limitation limits the possibility of an industry-standard wideband VLC dimming connection[22].

As a result, uninterrupted transmission is impossible. In addition to the problem of non-continuous transmission, when PWM brightness control is implemented, various faults occur. As a result, dimming VLC connections became unreliable [23]. RPO-OFDM was able to leverage the whole dynamic range of the LED, assuring full communication[24]. It has been demonstrated that it outperforms other O-OFDM schemes. The new signal format is based on multi-layer ACO-OFDM sequences that convey BCS data in the form of M−PPM.We demonstrate that the new OFDM technique can fully utilize the dynamic range of the LED while avoiding significant non-linear distortion in brightness adjustment [25]. The allowable brightness levels are determined by the series. They created an RPO-OFDM detector that can extract data from both sequences.

Using a modulation approach, the data that has to be conveyed is combined with the PWM signal's fading effects (carrier signal). As a result, decreasing the PWM duty cycle lowers average signal intensity and increases the likelihood of noise interference [26]. For the first time, VLC dimming control was carried out using straightforward digital modulation algorithms as PWM, PPM and PAM[27]. It is common to dim while keeping a steady communication link using straightforward OFDM-based methods like DCO-OFDM and ACOOFDM [28]. The data from the shutdown pulse, which occurs when the PWM pulse is zero, cannot be modulated using any of the aforementioned modulation techniques. Continuous transfer is therefore not carried out [29]. Additionally, in addition to the drawbacks of discontinuous transmission, there will be an increase in errors as a result of the introduction of PWM dimming [30]. As a result, the VLC communication link that uses dimming control becomes unreliable. RPO-OFDM, a contemporary strategy built on the OFDM system, was then unveiled in the year of 2015 [31]. To guarantee constant complete transmission, RPO-OFDM flips the polarity of the PWM pulses and makes use of the whole LED dynamic range [32]. Regarding BER [33], SNR, and data rate, studies [34] have shown that it performs better than other O-OFDM schemes [35]. The summary of the survey is tabulated as Table 1.

Problem Definition:

However, a significant design challenge preventing widespread use of VLC is figuring out how to integrate the widely-used PWM darkening technique with a stable, high-speed network connection. To maximise the LED's output, this study introduces a novel signal format called RPO-OFDM, which combines the rapid O-OFDM contact signal with the relatively slow PWM dimming signal. Not only does digital dimming result in less colour shift than analogue dimming, but it also offers considerable practical advantages in dimming thanks to simple duty cycle adap-tion. As a consequence, one of the goals of designing genuine VLC systems is to integrate OFDM and dimming control systems. When the light intensity is low, the duty cycle decreases, and just the "on" section of the PWM code is utilised to transmit the OFDM signal, leading to a reduced data rate. With RPO-OFDM, the data rate is not constrained by the PWM signal's frequency, nonlinear distortion of the O-OFDM communication signal is minimised, and the vast majority of the bit error power stays within the luminaire's brightness control range. In addition, RPO-OFDM offers a practical strategy for using commercially available LED drivers.

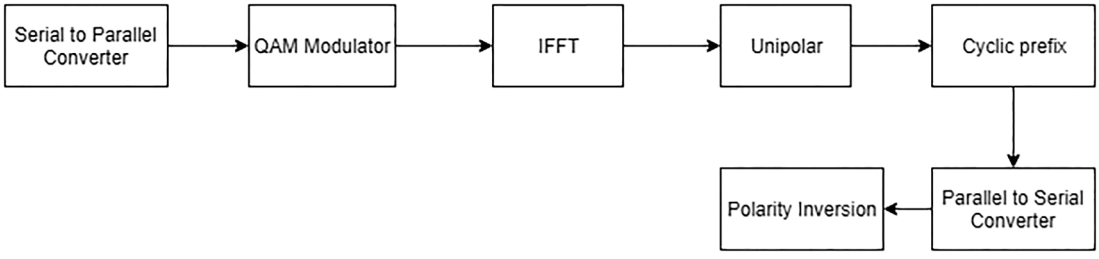

Fig. 2. RPO-OFDM Block Diagram.

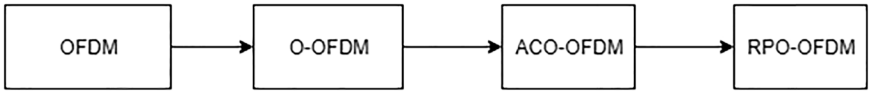

Fig. 3. RPO-OFDM Block Diagram.

Fig. 4. AWGN block insertion.

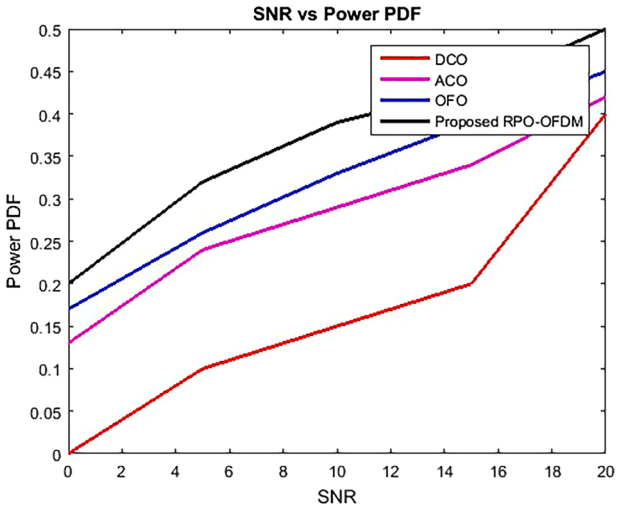

Fig. 5. Power PDF.

3. Proposed method

Using RPO-OFDM for dimming control in VLC [36], created a digital PWM dimming approach in this work. A Quadrature Amplitude Modulation (QAM) modulator uses a constellation diagram to map the transmitted O-OFDM symbols. RPO-OFDM is a modulation technology that combines the data into the light. The simulation process and results are covered in more detail in other sections. Simulations were done in MATLAB 2021(a).The optical attenuation of emitted light power and the perceived LED brightness of D and POFDM [38] are studied using simulations. The dimming level is a percentage of maximum brightness, with 100% being full brightness. IL = 0A, IH = 1A, and POFDM may be calculated using one ACO-OFDM code. The PWM-based method outperforms AM in spectrum efficiency and bit error performance. AM overlays the ACO-OFDM signal over a defined bias level. Therefore, the transmit LED's dynamic range is restricted, the ACOOFDM signal strength must be calibrated for each bias level, and the power is directly proportional to the brightness setpoint [39]. The recommended solution preserves the transmitted OFDM signal structure by not clipping the ACO-OFDM signal to the wider am-plitude range of the OFDM samples, providing the PWM signal utilises an LED with the complete dynamic range. Protecting the OFDM signal structure reduces generated clipping noise, enabling higher-order constellations (increased spectrum efficiency) or more reliable connections [40].To preserve QoS, the suggested solution isolates obfuscation from a wide range of performance, assuming optimal ACO-OFDM signal performance.

3.1. Optical-OFDM

It's critical to employ the O-OFDM module rather than the current OFDM module for research simulations in order to obtain superior results in terms of BER, SNR, and data rate. Optically modulated data is the subject of O-OFDM. LED drive signal practicality and positivity are requirements for O-OFDM [41]. The signal's entire reality is explained by hermitian symmetry. As a result, Hermitian symmetry at the IFFT input is required in order to realise the O-OFDM signal [1]. Fig. 3 below displays the O-OFDM transmitter's block diagram [42]. When using O-OFDM compliant equipment, demodulation is done in reverse order.

The RPO-OFDM transmitter block's block diagram is seen in Fig. 2.

A conversion of O-OFDM to RPOOFDM is depicted in Fig. 5. After clipping the O-OFDM signal's whole negative range to zero prior to the insertion of the CP, ACO-OFDM was produced.

By demanding Hermitian symmetry in the IFFT input, OFDM signals become O-OFDM symbols. The O-OFDM signal is clipped to zero and kept intact to form an ACO-OFDM bipolar signal. Inverting the PWM pulse polarity at zero produces the RPO-OFDM signal by superimposing the ACO-OFDM signal.

PWM darkening carrier signal and ACO-OFDM signal from PWM off pulse polarity reversal are used to transmit RPO-OFDM. To add and subtract iofdm(t) and ipwm(t), use the formula below [1]: PWM dimming signal pulse width (T) and period (Tpwm) are equal.

PWM pulses are "ON" and "OFF" (IH, IL). The on-and-off PWM pulses define PWM driving current. These observations and conclusions match the literature. Since PWM pulse trains drive the LED at a constant current level, duty cycle modifications significantly modify LED current. Where T is the pulse width and D is the duty cycle, the duty cycle is constant across the PWM period and depends on the dimming level.

RPO-OFDM modulated data is dimmed using 50% PWM duty cycle. A 50% duty cycle PWM contains modulated RPO-OFDM data. LEDs [4,7,12], and [37] are completely brightened by 100% duty cycle PWM. Lowering PWM duty cycle reduces light. BER rises and average signal strength falls. BER is somewhat reduced with FEC. 50% duty cycle PWM dimming BER versus SNR plot. Parallel-to-serial conversion of the dimming module's output before application to AWGN.

3.2. Additive white Gaussian noise (AWGN)

Receivers are not receiving AWGN in the transmitter output signal. The AWGN is depicted in Fig. 4 as being inserted in-between the transmitter and receiver. As an intrinsic noise substitute, add AWGN. Through a normal distribution across the frequency range, AWGN delivers constant power from the time domain.

Aspects of optical OFDM methods should be considered the design must be optimised to obtain optimum throughput at minimal transmission power while taking into account. As a result, it becomes possible to formulate an optimization problem that optimises throughput while adaptively decreasing transmits power based on the deterioration effects of noisy channels resulting to BER. By transmitting at a lower power, the performance of the system as a whole is further enhanced because higher transmit power results in power inefficiency. In order to achieve a suitable solution, the optimization problems objective function is again constrained by setting a power threshold for a single subcarrier.

Adaptive modulation systems, as opposed to conventional modulation schemes (DCO, ACO), offer parameters that can be adjusted in accordance with the fading channel. The fundamental query that so emerges is which parameters ought to be modified for greater performance. The demand to optimise effective throughput (data rate) has grown crucial given data usage trends and rising data rate requirements. Power, bit error rate, and transmission data rate (throughput) are all transmission factors that can be adjusted. Below equation specifies the starting (input) parameters for optimization/adaptation, and the output throughput is by,

$$\boldsymbol{b}_{thru} = \sum_{\gamma=1}^{\frac{N}{2}-1} \boldsymbol{b}_{\gamma,FLIP} \tag{1}$$

The power distribution of each subcarrier index is used to calculate BER approximations for MQAM.

$$\boldsymbol{BER}_{\gamma,FLIP} \approx 0.2\mathbf{exp}\left(-1.6\frac{\boldsymbol{P}_{\gamma,FLIP}}{2^{\boldsymbol{b}_{\gamma,FLIP}}-1}\boldsymbol{\xi}_{\gamma}\right. \tag{2}$$

The AWGN variance σ_{γ}^{2}, and the channel-to-noise ratio $\xi\gamma$ is defined as follows:

$$\xi_\gamma = \frac{|H_\gamma|^2}{\sigma_\gamma^2} \tag{3}$$

When (1) and (2) are put together, get:

$$b_{thru} = \sum_{\gamma=1}^{\frac{N}{2}-1} b_{\gamma,FLIP} \tag{4}$$

$$\nabla F(b) = \lambda \nabla c_i(b,p) \tag{5}$$

According to the Lagrangian multiplier, the objective function and restrictions create halting points where they contact and the gradient vectors of each are parallel to one another. When (5) is taken into account, the inequality constraint is changed to an equality constraint, and a non-negative marginal variable called $Si2\forall 1 \le i \le 2$ is added.

$$C_i(b,p,s) = c_i(b,p) + S_i^2 = 0 \forall 1 \le i \le 2 \tag{6}$$

Rewriting equation (6) as follows

$$\nabla F(b) = \lambda \nabla c_i(b,p,s) \tag{7}$$

From (7) directly follows the Lagrangian function $\mathscr{L}$ as:

$$L(b,p,s,\lambda) = F(b) - \lambda c_i(b,p,s) \tag{8}$$

The Lagrangian function is calculated by combining (7), (8); see also

$$L(b,p,s,\lambda) = \tau \sum_{\gamma=1}^{\frac{N}{2}-1} b_{\gamma,FLIP} - \lambda_1 \left[0.2 \sum_{\gamma=1}^{\frac{n}{2}-1} b_{\gamma,FLIP} \exp\left(-1.6 \frac{P_{\gamma,FLIP}}{2^{b_{\gamma,FLIP}} - 1} \xi_\gamma\right) - \mathrm{BER}_{\mathrm{thres}} \sum_{\gamma=1}^{\frac{N}{2}-1} b_{\gamma,FLIP} + S_1^2 \right] - \lambda_2 \sum_{\gamma=1}^{\frac{N}{2}-1} P_{\gamma,FLIP} - P_{thres} + S_2^2 \tag{9}$$

The system of equations f(ωj) with unknowns is given by the slope of the function. S1 = λ1 = 0S2 = λ2 = 0. The expanded technique results in a microcrystalline system with no singular solution are applied to the system. So, it is impossible to analytically solve the set of equations in (10). So, in an effort to create our own answer, try to apply unconstrained optimization approaches (numerical methods)

$$[H] = \nabla^2 L(b,p,s,\lambda) \tag{10}$$

The largest change in a given function's value typically moves in the direction of the slope because the slope of the Lagrange function, the first derivative test, specifies the stopping point. So, finding the maximum of the Lagrange function can be done with enough precision using the gradient. Basically, employ the Hessian matrix to locate spots that exactly match the optimum since, for finite optimization problems, travelling directions along the slope of the function may lead to infeasible regions. The unconstrained formulation can be applied by performing a second derivative test, which leads to a differential test.

As a result, the Hessian may be quickly calculated using well-known unconstrained techniques. While the Newton strategy performs best when ω*opt* is closer to the optimal solution ω*opt*, the steepest sane method converges when ω is far from ideal. Therefore, since BM more accurately converges from the previously computed Hessian matrix, using it to maximize throughput is adequate. This study's algorithm was carefully chosen because no other studies like it have used it because there wasn't any comparable literature at the time of the study.

Depending on how near the optimal value ω*opt* is, the BM technique uses the optimal stride component αj to determine the search direction at each iteration j. Iterations begin at a starting point o and a starting step size ho, resulting in a series of ωj points ω1,ω2, ω3,… convergent to a solution ωo.

The equations from the system (ω*j*) are used in the suggested approach for throughput optimization. Regarding given the starting values of ω0 and h0, compute the value of (ω*o*) such that ω1 = ω0 + h0, the ideal solution ω*op* optimal value ω*opt* iteratively converges from j. Set the maximum number of iterations to jmax and stop iterating if j doesn't converge to the ideal value from j = jmax to avoid iterative infinite loops.

Consequently, it will obtain optimised throughput bγ, pt, can resume the procedure and arrive at the optimal value from ω*opt*. The RPO (Reverse Polar Optical) OFDM scheme has been suggested for the coding convention, and Table 1′s algorithm illustrates it. A system of optical OFDM with N = 1024 subcarriers makes up the multicarrier scheme under consideration. The mean of the broadcast signal × is represented as a zero-Gaussian distribution, when the total number of subcarriers is adequate. Electrical and optical power's large variance 2 for N ≥ 64 are E(x2) and E(x) respectively. Directly, generated from the model equations are the simulation parameters for both the proposed technique and the traditional multi-carrier scheme. To limit the performance of the suggested strategy in optimising throughput while still adhering to standards and best practises, set the threshold BER and power at 10–4 and 0.1, respectively. The values of *v*1 = 0.5, v2 = 1, ϵ1 = ϵ2 = 10–6, and jmax = 102 are the parameters for the BM algorithm.

4. Results

This section shows RPO-OFDM dimmer control circuit simulation results with and without FEC codes like Reed Solomon and convolutional codes. This section discusses RPO-OFDM dimming circuit simulations with and without FEC codes like convolutional encoders and Reed Solomon. Simulations were done in MATLAB 2021(a).

L-layer ACO-OFDM modulates N = 256 subcarriers using 4-QAM.

BCS: 16-PPM is utilized to provide 15 brightness levels.

The sampling dynamic range of the RPO-OFDM signal is set from IL = 0 to IH = 1 and is presumed to be the same as that of the LED.

LED: Because the LED's modulation bandwidth is assumed to be greater than 2 MHz, the LED's electrical-optical conversion factor is constant across all subcarriers.

Noise: It is expected that when aliasing is removed, the noise in the snapshot has a bandwidth that corresponds to the intended signal. 0:001 represents its typical strength.

Power-Probability Density Function (PDF).

Fig. 5 shown a plot of the power's probability density function (PDF). For the purposes of calculating the power cost of the system, the chance of power values less than 0.85 was 85% for RPO and BMA, and 85% for power values less than 2, 2.5, and 3. 5 for ACO, OFO, and DCO, respectively. Comparing RPO-OFDM PDF to the research items, they

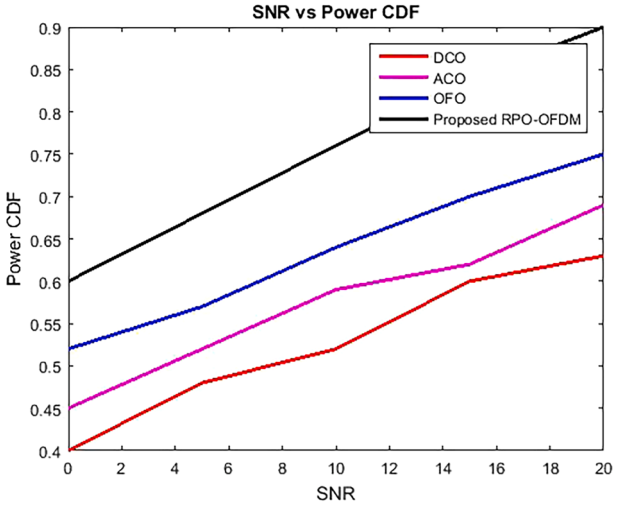

Fig. 6. Power CDF.

demonstrated superior power distribution and higher power efficiency. When compared to RPO-OFDM, the power needed to drive the models by OFO, ACO, and DCO schemes is 2.2, 1.8, and 4.9 greater, respectively. As a result, implementation costs and design complexity are higher. The high power and low complexity of RPO-OFDM, which was optimised in this work, make it the ideal choice for conventional approaches.

Power-Cumulative Distribution Function (CDF).

The power's CDF plot is displayed in Fig. 6 for viewing pleasure. DCO, ACO, and PSO require higher power values than the RPO-OFDM approaches are suggested for a given cumulative probability value. For RPO-OFDM, the chance of a power value less than 0.85 is considered to be 85% of the power cost of the scheme, whereas for ACO, PSO, and OFO, the probability of a power value less than 1.5, 2, and 3. 5 respectively, is considered to be 80% of the power cost. RPO-OFDM CDF are more energy-efficient in comparison and have advantages in power distribution. When compared to RPO-OFDM, the power needed to drive the models by OFO, ACO, and DCO schemes is 2.2, 1.8, and 4.9 greater, respectively. As a result, implementation costs and design complexity are higher. The PDF of the value and the CDF plot's slope are identical.

BER vs SNR.

Fig. 7 contrasts the 2 V 16QAM subcarrier modulation BER performance of various methods. RPO, DCO, ACO, and OFO achieve 1.654 × 10–3, 1.843 × 10–2, 6.3 × 10–2, and 3.189 × 10–2 BER performance, respectively, at 15 dB SNR. By achieving reduced BER for a given SNR, the suggested (RPO) algorithm outperforms traditional approaches.

This project aims to build a VLC connection with minimal LED light output and drastically lower BER while using less electricity. Because 100% was the LED's maximum brightness, the PWM duty cycle was adjusted to produce several brightness ranges. Adjusting the PWM duty cycle changes LED brightness. The following equation showed how PWM duty cycle affects LED brightness.

We achieved a 10^{-3} BER at 15.6 dB without convolutional coding. When CC was added, we got a BER of 10^{-3} with an SNR of 15, which is adequate for VLC attenuation. SNR improves somewhat. CC management at 75% duty cycle decreased power by 0.6 dB. To study how VLC dimming affects BER and SNR, PWM duty cycle was dropped to 50%. RPO-OFDM data was overlaid on a 50% duty cycle PWM pulse, as shown.

At 50% duty cycle reduction, RPO-OFDM modulated data had a 10–0.8 higher BER than 75% pulsed PWM. The BER error rate without convolutional coding is 10–3 at 16 dB. With CC, we got a BER of 10^{-3} and SNR of 15. VLC accepts 10^{-3} BER for attenuation. SNR improves marginally, however performance suffers from dimming the CC at 50%

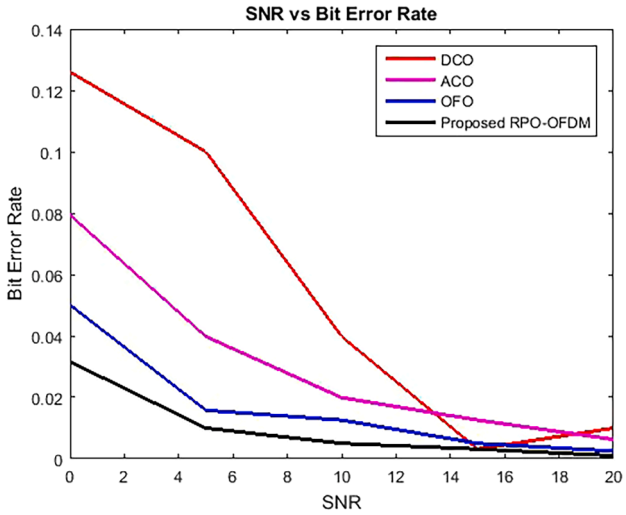

Fig. 7. SNR vs Bit Error Rate.

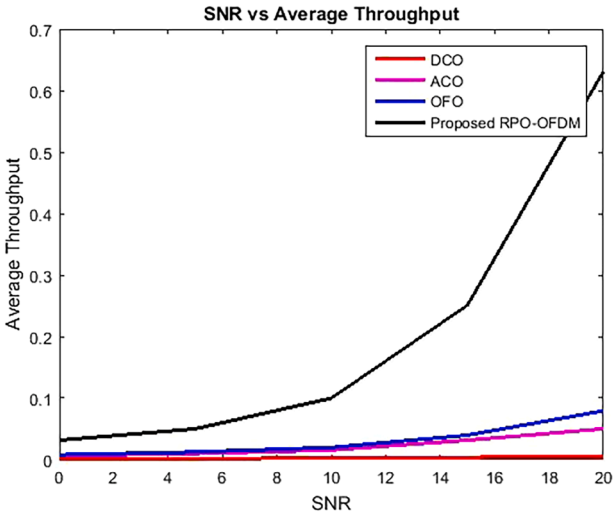

Fig. 8. Average Throughput.

duty cycle.

To study how VLC dimming affects BER and SNR, PWM duty cycle was dropped to 35%. RPO-OFDM data was overlaid on a 35% duty cycle PWM pulse, as shown. The SNR needed to create 10^{-3} BER for RPO-OFDM modulated data with a 35% fill factor was 14 dB higher than a 50% PWM pulse.

Average Throughput.

With and without power limitation, the average throughput and average SNR plots are shown in Fig. 8 for $\tau = 0.5$. It appears that average SNR rise together with average throughput. Since almost all of the subcarriers are utilised when the SNR is above 25 dB, the RPO algorithm maintains a constant average transmit power, ensuring power efficiency while increasing average throughput. Average throughput marginally decreases when power limiting is used, although performance remains similar when SNRs are lower. At low SNR, less power is required, leading in a reduced transmit power and equivalent average throughput with and without the power limitation. As SNR grows, average throughput decreases somewhat because the total subcarrier transmit power exceeds the charging limit power. In light of this, RPO maximises throughput while meeting power constraints.

5. Discussion

The study created a PWM digital dimming technique that uses Visible Light Communications (VLC) RPO-OFDM to manage dimming. The QAM modulator maps the O-OFDM symbols that will be sent in the towers. Data is embedded in light via RPO-OFDM modulation. The dimmer transmitter's random data generator comes first. The random data generator prevents lengthy sequences of 0′s and 1′s from interrupting subsequent time requests. Data is converted from parallel to serial before entering the FEC encryption block. QAM modulators convert serial data bits into symbols. Mappers assign symbols to IFFT (subcarrier) input bins. IFFT is used to convert the frequency domain O-OFDM symbol to the time domain signal. The unipolar process, like ACO-OFDM, generates unipolar OOFDM symbols based on subcarrier assignment. To prevent intersymbol interference, a fixed-length periodic prefix (CP) precedes the polarity transition. D, the dimming level, activates the polarity switch. The suggested method modulates the LED driver's dimming signal current with the polarity-modulated O-OFDM analogue signal current following the RPOOFDM modulator to drive brightness.

6. Conclusion

Here, presents a novel signal conditioning approach in this study for high-throughput visible spectrum applications. Utilizing Lagrangian multipliers and the Berlekamp-Massey algorithm, the throughput improvement strategy is based on dynamically adjusting transmission parameters to channel circumstances based on bit error rate (BER) performance. This work demonstrates that 16 QAM, which has 16 potential signal combinations and an effective symbol throughput of 9 bits/symbol, can be used in broadband applications for VLC with SNR greater than 25 dB. ACO and OFO conventional methods cannot be employed in communication systems for the majority of use cases, as shown by the observation that the abrupt decline of BER response can track the effect of channel noise on the system. It is discovered that the proposed RPO approach is more responsive than BER, adaptively handles channel impacts, and has the benefit of higher overall throughput. According to our research, the aforementioned proposed RPO algorithm surpasses the spectrum-efficient DCO scheme in terms of throughput performance by roughly 3% and the energy- and spectrum-efficient OFO and ACO schemes by 5%. Additionally, it appears that the proposed RPO technique performs much better than the adaptive RF-based scheme. By increasing performance by 65%, 27%, and 22% above conventional algorithms, RPO outperforms them. The suggested technique outperforms traditional algorithms in terms of enhancing average signal-to-noise ratio (SNR), while also maximising throughput while subject to total transmission power and average bit error rate (BER) restrictions. Additionally, at low bit error rate (BER) thresholds the algorithm outperforms traditional signal conditioning algorithms (DCO, ACO, and OFO). The paper contemplated the high-performance signal conditioning methods and standards for visible light communication, which will benefit the communication industry. FEC codes, such concatenated RS-CC, help to improve BER. The RS code is only applied, nevertheless, to duty cycles where 100% of the time is spent in operation. Future investigations may find that pairing RS with CC greatly enhances the BER obtained at various dimming levels. The needed minimum LED brightness for VLC communication now stands at less than 48%. Future experiments can explore various CC and RS speeds to reduce BER. Future studies could examine how employing various communication channels (such Reyleigh, Multipath, etc.) affects controlling VLC dimming. Future development may include include the hardware needed to implement the dimming circuit. FEC codes such as serial RS-CC improve BER. However, on the BER load cycle, the RS sign was only improved to 100%. By connecting RS with CC, further research can greatly enhance the obtained BER for varied dimming ranges. The minimum LED brightness necessary to interact with VLC is therefore less than 45%. Different CC and RS ratios can be tested in the future to attain a lower BER. Future research can also look into the effects of different communication channels, such as Rayleigh, Multipath, and so on, on VLC brightness control. A realistic hardware version of the dimming circuit may also be developed in the future.

Funding.

This research was supported by Princess Nourah bint Abdulrahman University Researchers Supporting Project Number (PNURSP2023R97), Princess Nourah bint Abdulrahman University, Riyadh, Saudi Arabia.

Declaration of Competing Interest

The authors declare that they have no known competing financial interests or personal relationships that could have appeared to influence the work reported in this paper.

Acknowledgement

Princess Nourah bint Abdulrahman University Researchers Supporting Project Number (PNURSP2023R97), Princess Nourah bint Abdulrahman University, Riyadh, Saudi Arabia.

References

[1] Ibhaze E, Orukpe PE, Edeko FO. Visible light channel modeling for high-data transmission in the oil and gas industry. Journal of Science and Technology 2020; 12(2):46–54.
[2] Lian J, Gao Y, Lian D. Variable pulse width unipolar orthogonal frequency division multiplexing for visible light communication systems. IEEE Access 2019;7: 31022–30.
[3] Zheng Z, Jiang S, Feng R, Ge L, Gu C. Survey of Reinforcement-Learning-Based MAC protocols for wireless ad hoc networks with a MAC reference model. Entropy 2023;25:101. https://doi.org/10.3390/e25010101.
[4] Ibhaze AE, Orukpe PE, Edeko FO. Li-Fi prospect in internet of things network. FICC2020, advances in intelligent systems and computing. Cham, Switzerland: Springer Nature Switzerland AG 2020;1129:272–80.
[5] Shahi S, Tuninetti D, Devroye N. The strongly asynchronous massive access channel. Entropy 2023;25:65. https://doi.org/10.3390/e25010065.
[6] Huang X, Yang F, Zhang H, Ye J, Song J. Subcarrier and power allocations for dimmable ehanced ADO-OFDM with iterative interference cancellation. IEEE Access 2019;7:28422–35.
[7] Pereira FRF, Mancini S. Entanglement-Assisted quantum codes from cyclic codes. Entropy 2023;25(1):37. https://doi.org/10.3390/e25010037.
[8] Agboje OE, Idowu-Bismark OB, Ibhaze AE. Comparative analysis of fast fourier transform and discrete wavelet transform based MIMO-OFDM. International Journal on Communications Antenna and Propagation (IReCAP) 2017;7(2): 168–75.
[9] ZhaochengWang , Tianqi Mao, and Qi Wang. 2017. Optical OFDM for visible light communications. IEEE 13th International Wireless Communications and Mobile Computing Conference (IWCMC), Valencia, Spain, 1190 - 1194.
[10] Cai Z, Lin L, Zhou X. Learn Quasi-Stationary distributions of finite state markov chain. Entropy 2022;24:133. https://doi.org/10.3390/e24010133.
[11] Palanisamy S, Thangaraju B. Design and analysis of clover leaf-shaped fractal antenna integrated with stepped impedance resonator for wireless applications. International Journal of Communication Systems 2022;35(11):e5184.
[12] Kavitha T, Sonika M, Prathyusha NL, Raj VT. Modelling of oFDM modulation technique in HF radio band using MATLAB. Journal of Optical August 2022. Communications.
[13] Minseok Yu, Chun H. RCS-OFDM enabling full brightness control with power-efficient visible-light communication. Optics Letters 2022;47:277–80. https://opg.optica.org/ol/abstract.cfm?URI=ol-47-2-277.
[14] Nivethitha T, Palanisamy SK, MohanaPrakash K, Jeevitha K. Comparative study of ANN and fuzzy classifier for forecasting electrical activity of heart to diagnose Covid-19. Materials Today: Proceedings 2021;45:2293–305. https://doi.org/10.1016/j.matpr.2020.10.400.
[15] Palanisamy S, Thangaraju B, Khalaf OI, Alotaibi Y, Alghamdi S, Alassery F. A novel approach of design and analysis of a hexagonal fractal antenna array (HFAA) for Next-Generation wireless communication. Energies 2021;14(19):6204.
[16] Palanisamy S, Thangaraju B, Khalaf OI, Alotaibi Y, Alghamdi S. Design and synthesis of Multi-Mode bandpass filter for wireless applications. Electronics 2021; 10(22):2853. https://doi.org/10.3390/electronics10222853.
[17] Yao Y, Xiao K, Xia B, Gu Q. Design and analysis of rotated-QAM based probabilistic shaping scheme for rayleigh fading channels. IEEE Transactions on Wireless Communications May 2020;19(5):3047–63. https://doi.org/10.1109/TWC.2020.2970007.
[18] SatheeshKumar,&Balakumaran T.. Modeling and simulation of dual layered u-slot multiband microstrip patch antenna for wireless applications. Nanoscale Reports 2021;4(1):15–8. https://doi.org/10.26524/nr.4.3.
[19] AngurajKandasamy, SaravanakumarRengarasu, Praveen KittiBurri, SatheeshkumarPalanisamy, K. Kavin Kumar, Aruna Devi Baladhandapani, Samson AlemayehuMamo, "Defected Circular-Cross Stub Copper Metal Printed Pentaband Antenna", Advances in Materials Science and Engineering, vol. 2022, Article ID 6009092, 10 pages, 2022. https://doi.org/10.1155/2022/6009092.
[20] Palanisamy S. Predictive Analytics with Data Visualization. Journal of Ubiquitous Computing and Communication Technologies 2022;4(2):75–96. https://doi.org/10.36548/jucct.2022.2.003.
[21] Kavitha T, Kumar AP, Sowmith A. Performance analysis of single side band orthogonal frequency division multiplexing in radio over fiber system with direct and external modulation schemes. Journal of Optical Communications 2019;Q3. https://doi.org/10.1515/joc-2018-0231.
[22] Li Y, Deng Y, He J, He S, Chen L. DFT-spread combined with clipping method to reduce the PAPR in VLC-OFDM system. Optoelectronics Letters 2017;13(3): 229–32.
[23] Kumar S, Tomar P, Shukla A. Effectiveness of OFDM with antenna diversity. In: IEEE International Conference on Communication, Control and Intelligent Systems; 2015. p. 172–5.
[24] Kavitha, T., Maheswaran, G., Maheswaran, J., & Pappa, C. K. (2023). Optical network on chip: Design of wavelength routed optical ring architecture. Bulletin of Electrical Engineering and Informatics, 12(1, February), 167–175. 10.11591/eei.v12i1.4294.
[25] Amit Grover A. Manikandan, vivek soi, anu sheetal, mehtab singh, realisation of white LED using fiber-based hybrid photonic structures, optoelectronics and advanced materials - rapid communications, 15, 11–12. November-December 2021;2021:521–7.
[26] Sam PJC, Surendar U, Ekpe UM, Saravanan M, Satheesh Kumar P. A Low-Profile Compact EBG Integrated Circular Monopole Antenna for Wearable Medical Application. In: Malik PK, Lu J, Madhav BTP, Kalkhambkar G, Amit S, editors.

Smart Antennas. EAI/Springer Innovations in Communication and. Computing. Springer; 2022.
[27] Manikandan A, Nirmala V, Sheikdavood K. STBC-OFDM downlink baseband receiver. International Journal of American Eurasian Network for Scientific Information 2014;8(19):69–74.
[28] Chen J, You X, Zheng H, Yu C. "MPPM dimming control for OFDM-based visible light communication systems", in. IEEE International Conference on Communication Systems (ICCS) 2014;2014:268–72.
[29] Satheesh Kumar, P., Jeevitha, Manikandan (2021). Diagnosing COVID-19 Virus in the Cardiovascular System Using ANN. In: Oliva, D., Hassan, S.A., Mohamed, A. (eds) Artificial Intelligence for COVID-19. Studies in Systems, Decision and Control, vol 358.Springer, Cham.https://doi.org/10.1007/978-3-030-69744-0_5.
[30] Iqbal Jebril & P. Dhanaraj & Ghaida Muttashar Abdulsahib & SatheeshKumar Palanisamy & T.Prabhu & Osamah Ibrahim Khalaf, 2022. "Analysis of Electrically Couple SRR EBG Structure for Sub 6 GHz Wireless Applications," Advances in Decision Sciences, Asia University, Taiwan, vol. 26(Special), pages 102-123, December.
[31] E. Suganya, T. Prabhu, Satheeshkumar Palanisamy, Praveen Kumar Malik, Naveen Bilandi, Anita Gehlot, "An Isolation Improvement for Closely Spaced MIMO Antenna Using λ/4 Distance for WLAN Applications", International Journal of Antennas and Propagation, vol. 2023, Article ID 4839134, 13 pages, 2023. 10.1155/2023/4839134.
[32] Chen S, Zhao J. The requirements, challenges, and technologies for 5G of terrestrial mobile telecommunication. IEEE Communications Magazine 2014;52(5):36–43.
[33] Dhanasekaran S, Ramesh.J,. Channel estimation using spatial partitioning with coalitional game theory (SPCGT) in wireless communication. Wireless Networks 2021;27:1887–99. https://doi.org/10.1007/s11276-020-02528-4.
[34] P. S. Kumar, S. Boopathy, S. Dhanasekaran and K. R. G. Anand, "Optimization of Multi-Band Antenna for Wireless Communication Systems using Genetic Algorithm," 2021 International Conference on Advancements in Electrical, Electronics, Communication, Computing and Automation (ICAECA), 2021, pp. 1-6, doi: 10.1109/ICAECA52838.2021.9675686.
[35] Suganyadevi K, Nandhalal V, Palanisamy S, Dhanasekaran S. Data security and safety services using modified timed efficient stream Loss-Tolerant authentication in diverse models of VANET. international Conference on Edge Computing and Applications (ICECAA) 2022;2022:417–22. https://doi.org/10.1109/ICECAA55415.2022.9936128.
[36] Tang Z, Xie H, Du C, Liu Y, Khalaf OI, Allimuthu UK. Machine learning assisted energy optimization in smart grid for smart city applications. J Inter Net 2022;22 (Supp03).
[37] S. Goswami, A. K. Sagar, P. Nand and O. I. Khalaf, "Time Series Analysis Using Stacked LSTM Model for Indian Stock Market," 2022 IEEE IAS Global Conference on Emerging Technologies (GlobConET), Arad, Romania, 2022, pp. 399-405, doi: 10.1109/GlobConET53749.2022.9872386.
[38] Shivappriya, S.N., Palanisamy, S., Mohammed Shareef, A., Ali Zearah, S. (2023). Significance of Literacy in Minimizing Infant Mortality and Maternal Anemia in India: A State-Wise Analysis. In: Swaroop, A., Kansal, V., Fortino, G., Hassanien, A. E. (eds) Proceedings of Fourth Doctoral Symposium on Computational Intelligence . DoSCI 2023. Lecture Notes in Networks and Systems, vol 726. Springer, Singapore. https://doi.org/10.1007/978-981-99-3716-5_73.
[39] Palanisamy, S., Nivethitha, T., Alhameed, M.R., Udhayakumar, A., Hussien, N.A. (2023). Urban Wastewater Treatment for High Yielding in Agriculture Through Smart Irrigation System. In: Swaroop, A., Kansal, V., Fortino, G., Hassanien, A.E. (eds) Proceedings of Fourth Doctoral Symposium on Computational Intelligence . DoSCI 2023. Lecture Notes in Networks and Systems, vol 726. Springer, Singapore. https://doi.org/10.1007/978-981-99-3716-5_52.
[40] Xue, X.; Shanmugam, R.; Palanisamy, S.; Khalaf, O.I.; Selvaraj, D.; Abdulsahib, G. M.A Hybrid Cross Layer with Harris-Hawk-Optimization-Based Efficient Routing for Wireless Sensor Networks. Symmetry 2023, 15, 438.10.3390/sym15020438.
[41] A. P. Mukti, L. Lusiana, D. Titisari, and S. Palanisamy, "Performance Analysis of Twelve Lead ECG Based on Delivery Distance Using Bluetooth Communication", j. electron.electromedical.eng.med.inform, vol. 5, no. 1, pp. 46-52, Jan. 2023.
[42] S D, Palanisamy SatheeshKumar, Hajjej F, Khalaf OI, Abdulsahib GM, S R. Discrete fourier transform with denoise model based least square wiener channel estimator for channel estimation in MIMO-OFDM. "Discrete fourier transform with denoise model based least square wiener channel estimator for channel estimation in MIMO-OFDM" Entropy 24 2022;24(11):1601.